LA-UR- 96-1406

CONF-960401--48

Title: TRIBOLOGY STUDIES OF ORGANIC THIN FILMS BY SCANNING FORCE MICROSCOPY

Author(s):
G. Bar
S. Rubin
A. N. Parikah
B. I. Swanson
T. A. Zawodzinski

Submitted to: Materials Research Society

Los Alamos
NATIONAL LABORATORY

Form No. 836 R5
ST 2629 10/91

TRIBOLOGY STUDIES OF ORGANIC THIN FILMS BY SCANNING FORCE MICROSCOPY

G. BAR*, S. RUBIN**, A. N. PARIKH**, B. I. SWANSON**, T. A. ZAWODZINSKI**
*Freiburger Materialforschungszentrum, FMF, Albert-Ludwigs University, Stefan-Meier-Str. 21, 79104 Freiburg, Germany, gbar@fmf.uni-freiburg.de
**Los Alamos National Laboratory, Los Alamos, NM 87545, USA

ABSTRACT

Using the micro-contact printing method we prepared patterned self-assembled monolayers (SAMs) consisting of methyl-terminated alkanethiols of different chain lengths. The samples were characterized using lateral force microscopy (LFM) and the force modulation technique (FMT). In general, higher friction is observed over the short chain regions than over the long chain regions when a low or moderate load is applied to the SFM tip. For such cases the high friction (short chain) regions are also "softer" as measured by FMT. At high loads, a reversal of the image contrast is observed and the short chain regions show a lower friction than the long chain regions. This image contrast is reversible upon reduction of the applied load.

INTRODUCTION

The use of organic thin films as lubricants on solid surfaces is important in many modern technologies including magnetic storage and micromachines [1, 2]. Langmuir-Blodgett (LB) films and self-assembled monolayers (SAMs) are attractive candidates for lubricant layers and for model studies of lubrication because of their strong adsorption to the surface. The recent interest on the properties of LB films and SAMs has been also motivated by their potential applications in sensors [3], non-linear optical devices [4], lithography [5] and microelectronics [6].

Recently, considerable interest has been shown in characterization of LB-films and SAMs (and in particular patterned SAMs) using scanning force microscopy (SFM). In particular, it has been demonstrated that lateral force microscopy (LFM), which measures the friction forces between the tip and the sample surface, can distinguish between chemically different surface regions. Such experiments providing material-contrast imaging are relevant to applications involving lubrication, adhesion and wetting. Knowing the interaction leading to different friction forces between the SFM tip and the sample surface is essential for the understanding of the image contrast relating the contrast to the tribological surface properties. Unfortunately, the interpretation of the experimental data is complicated because the mechanisms underlying the image contrast are not yet completely understood. As a consequence, conclusions based on results reported to date are far from being unequivocal. The LFM image contrast observed between different domains of phase-separated domains is believed to be due to differences in the mechanical properties of the LB domains, i. e. elastic compliance[7]. The frictional properties of SAMs of methyl-terminated alkylsilanes of different chain lengths on mica substrates are seen to depend strongly on the chain length [8] such that higher friction was observed for short chain lengths. This effect was attributed to disorder in the layers formed by molecules with short chain length. On the other hand recent investigations of patterned SAMs consisting of regions of alkanethiols with chemically different terminal groups suggested that the friction contrast observed in LFM might be dominated by the chemical identity of the end groups of the surface and tip [9-10]. Thus, there is a need to study in more detail the effects of order, packing, crystallinity and chemical identity of the terminal end groups on the observed frictional contrast in LFM.

In this paper, we discuss the LFM image contrast between different regions of a patterned SAM consisting of alkanethiols having the same terminal end group, $-CH_3$, but different chain lengths. We investigate in particular the correlation between the observed frictional contrast and the measured local elastic properties of the different regions of the SAM using the force modulation technique (FMT). FMT is based on the principle that the vertical force between the SFM tip and the sample surface is modulated by oscillating the probe and the relative elasticity of the sample is measured by recording the amplitude of the tip deflection versus position over

the sample [11-12]. We show that the frictional contrast between the short and the long chain regions strongly depends on the applied load.

EXPERIMENT

Materials: The silicon wafers were obtain from Semiconductor Processing Co. The gold surfaces were prepared by sputter deposition of 10 nm of titanium, followed by sputter deposition of 100 nm of gold, on the native layer of the silicon oxide. The gold and the titanium purity was 99.999%. Octadecyl mercaptan (C18), hexadecyl mercaptan (C16), nonyl mercaptan (C9) and heptyl mercaptan (C7) were obtained from Aldrich and were used without further purification. The micro-contact printing process was applied as described elsewhere[13].

Instruments: A commercial Digital Instruments Nanoscope III was used for the SFM experiments. The experiments reported here were carried out in air under ambient conditions. The measurements were performed with commercial Si cantilevers with nominal force constants C = 0.02 - 0.1 N/m and commercial Si_3N_4 cantilevers with nominal force constants C = 0.06 - 0.12 N/m. Topographic ("height") images were obtained in the constant force mode and simultaneously recorded with the friction maps which were obtained in the lateral force mode (LFM). The elasticity measurements, performed using the force modulation technique (FMT), were obtained simultaneously with topographic images. The data are presented as gray coded images such that bright areas correspond to higher regions in topographic images, higher friction in LFM images and softer regions in FMT images.

RESULTS

Figure 1 shows the SFM images of a patterned SAM sample on gold consisting of C18 (circular structure) and C7 arrays (surrounding the circles). The sample was prepared by first stamping the C18 component using a master consisting of circles (approx. 3 μm in diameter) and then exposing the stamped sample to C7 solution. The topography image (Figure 1a) shows clear image contrast between the more elevated C18 regions (bright gray) and the C7 surroundings. We measured ≈ 0.8 nm as height difference between the C18 and C7 surface regions which is in reasonable agreement with the expected value of 1 nm. One should note, however, that an exact measurement of the height difference is difficult due to the different penetration of the SFM tip into the C18 and C7 regions (see discussion of the local elastic properties below).

Figure 1b shows the LFM image (friction map) recorded simultaneously with the topography image shown in Figure 1a. In the LFM mode, very good contrast is observed between the circular C18 regions and the surrounding C7. The LFM map shows higher friction (bright gray) over the short chain C7 regions and lower friction over the long chain C18 regions (circles). The image presented was obtained applying a low load (≈16 nN)[14]. As shown below, the image contrast depends strongly on the force the tip exerts on the sample surface. Similar images were observed for patterned samples consisting of C18 and C9 arrays, C16 and C7 arrays and C16 and C9 arrays (data not shown). In all cases a higher frictional force was recorded over the short chain regions than over the long chain regions when a low or moderate load was applied (up to ≈ 190 nN).

Figure 1c shows the FMT image (elasticity map) of the patterned SAM sample. Imaging the patterned SAMs under ambient conditions produced contrast between the C18 regions (bright circles) and the C7 regions (dark surroundings). Bright regions correspond to softer sites which absorb more of the cantilever's energy, causing a reduced cantilever response and lower amplitudes. Figure 1c shows that the C7 surface regions are "stiffer" than the C18 circles. The same type of elasticity maps were observed for patterned samples consisting of C18 and C9 arrays, C16 and C7 arrays as well as for C16 and C9 arrays (data not shown). In all cases the short chain regions appeared "stiffer" than the long chain surface regions as measured by FMT. Studies of patterned SAMs consisting of surface regions with different chemical functionalities showed that the LFM image contrast generally seems to correlate with the surface free energy of the arrays [9, 10, 15]. Higher friction has been observed over the hydrophilic-COOH, or -OH terminated surface regions than over the hydrophobic $-CH_3$ terminated areas. However, these studies did not clarify to which extend other factors such as packing and disorder contribute to

Figure 1: SFM images of a patterned C18/C7 alkanethiol SAM on gold. (a) Topographic image. The horizontal bar corresponds to 10 μm and is representative for all images. The gray scale corresponds to a z-scale of 10 nm. (b) LFM image showing the friction map. Dark regions (C18) correspond to lower friction and bright regions (C7) to higher friction. (c) FMT image showing the local elasticity. Bright regions (C18) correspond to "softer" areas and dark regions (C7) to "stiffer" areas.

the observed image contrast. Contact angle measurements do not show pronounced differences between the short and long alkanethiols[16]. Thus one must conclude that the image contrast observed in the friction map (Figure 1b) originates from factors such as disorder and packing rather than from surface free energy/hydrophobicity. A recent study of the chain length dependence of the frictional properties of alkylsilane SAMs on mica showed that friction forces strongly depend on the length of the alkyl chains, being higher for the short chains, in agreement with our study [8]. The observed dependence of the friction forces on the chain length could be explained by a much higher alkyl chain disorder in the short chain SAMs. FTIR data suggest that SAMs of short chain alkanethiols ($n < 10$) have liquid-like chains packed at lower densities than their longer chain counterparts [17]. Thus, the possibility of differences in surface coverage should also be taken into account.

Our data show that the friction maps correlate with the local elasticity maps: the long chain arrays exhibit lower friction and are "softer" than the short chain regions. A similar correlation was reported for patterned SAMs consisting of chemically different arrays, i.e. -COOH and $-CH_3$ terminated alkanethiols, where the high friction -COOH regions appeared to be "stiffer"[10]. In the case of phase-separated LB films, a different correlation was observed: higher friction was observed for the "softer" fluorocarbon domains than for the "stiffer" hydrocarbon domains[12]. In that case, however, the fluorocarbon domains consisted of multilayers, the fluorocarbons sitting on top of the hydrocarbon monolayer. This seems to be important if the thickness of the organic film and the substrate plays a role. The liquid-like short chain alkanethiols are expected to be softer; however, one must take into account that the oscillating tip in FMT might "feel" the underlying substrate. In that case the short chain regions would appear "stiffer" as detected by FMT since the tip may penetrate more easily through the organic monolayer through the substrate. We note, however, the same type of image contrast was observed even with very small load and small oscillating amplitude.

We now turn to a study of patterned SAMs consisting of arrays of alkanethiols quite similar in chain length. This is assumed to minimize the effects arising from different film thickness and surface coverage. We prepared and investigated SAMs consisting of C18 circular regions and C16 regions surrounding the circles. Figure 2a shows the SFM topography image, which exhibits little image contrast. This is not surprising since the height difference between the C18 and C16 surface regions should be on the order of 0.2 nm. Figure 2b shows the friction map (LFM image) of the patterned SAM. The LFM image shows very good image contrast between the C18 and C16 surface arrays. Higher friction is observed over the C16 surface regions (bright gray) surrounding the C18 circles (dark gray), irrespective of which of the two components was

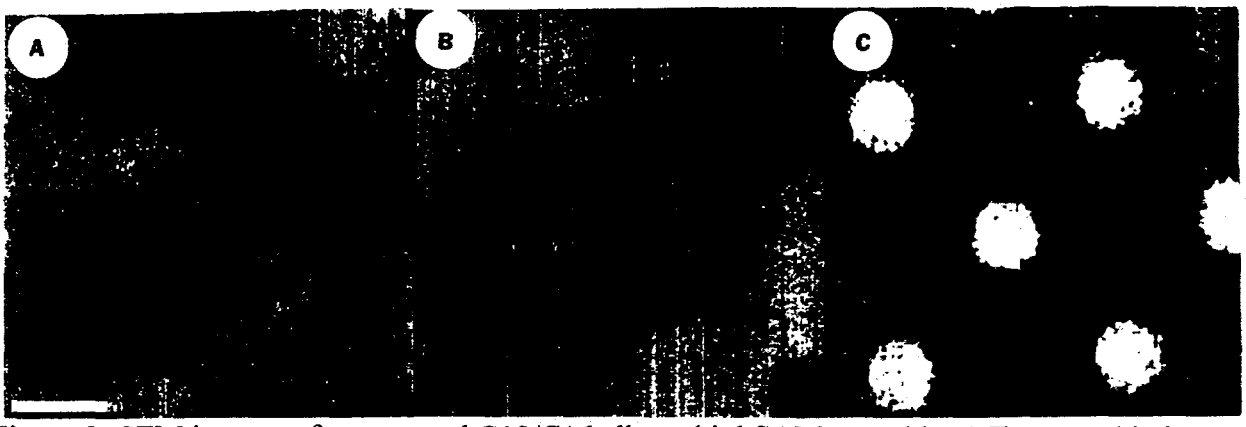

Figure 2: SFM images of a patterned C18/C16 alkanethiol SAM on gold. (a) Topographic image. The horizontal bar corresponds to 5 μm and is representative for all images. The gray scale corresponds to a z-scale of 10 nm. (b) LFM image showing the friction map. Dark regions (C18) correspond to lower friction and bright regions (C16) to higher friction. (c) FMT image showing the local elasticity. Bright regions (C18) correspond to "softer" areas and dark regions (C16) to "stiffer" areas.

adsorbed by stamping or from solution. This result is quite remarkable since it indicates that friction contrast can be observed between alkanethiol surface regions which differ by just two CH_2 groups: lower friction is always observed over the long chain surface regions. Figure 2c shows the FMT image (elasticity map) of the patterned SAM sample consisting of the C18 circular surface regions and their C16 surroundings. It shows that the C16 surface regions are "stiffer" than the C18 circles, again, independent of which component was stamped and which adsorbed from solution. Thus, as in the case of the patterned SAM consisting of quite different alkanethiol chain regions (e.g. C18 and C7), the short chain regions appeared "stiffer" than the long chain surface regions as measured by FMT.

It is instructive to explore the friction image dependence on the applied load. Figure 3 shows a

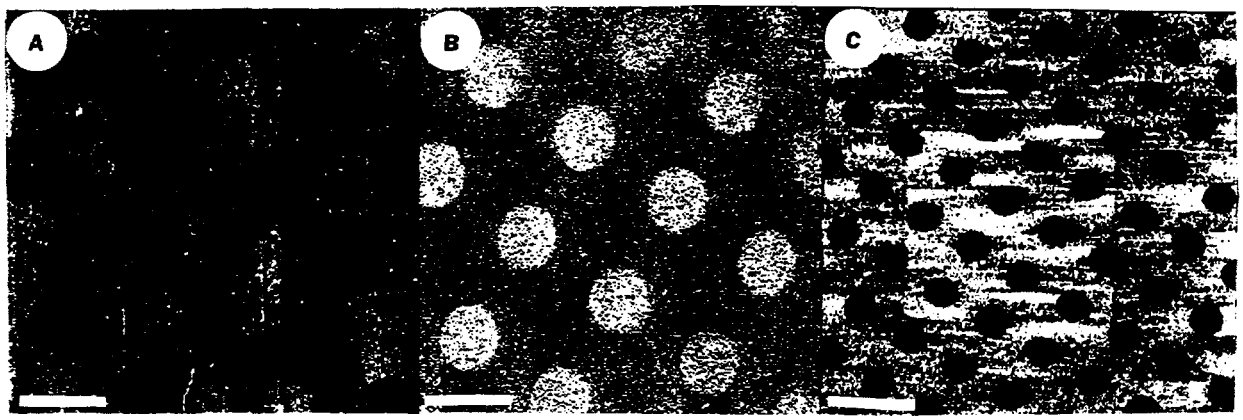

Figure 3: LFM images of a patterned C18/C7 alkanethiol SAM on gold. The horizontal bar corresponds to 5 μm in (a) and (b), and to 10 μm in (c). (a) LFM image recorded with a low load of 16 nN. The C18 regions show a lower friction (dark gray) than the C7 regions (bright gray) (b) LFM image recorded with a high load of 230 nN. The C18 regions show now a higher friction (bright gray) than the C7 regions (dark gray). (c) LFM image of a bigger area which has been previously scanned with a high force recorded with a low load of 11 nN. Now the C18 regions show again a lower friction (dark gray) than the C7 regions (bright gray).

series of LFM images for a patterned SAM sample consisting of C18 circular regions and C7 surroundings obtained with different loads. Figure 3a shows the friction map recorded applying a load of approx. ≈ 16 nN. As discussed above, lower friction is observed over the C18 surface regions (dark gray) than over the C7 surface regions at low load. Figure 3b shows the friction map of the same surface region recorded applying a much higher load of ≈ 230 nN. Above a certain threshold, a reversal of the LFM image contrast is observed. At high loads lower friction is observed over the short chain C7 region (dark gray) and higher friction over the long chain C18 regions (bright gray). One might expect that at high loads, destruction of the adsorbed organic surface layers would occur. However, we observed that the frictional contrast obtained at different loads was reversible. Figure 3c shows the LFM image acquired with a low load of a surface region which has been previously scanned with a high load. One can clearly recognize the rectangular surface region which has been scanned with higher loads. But nevertheless, the original image contrast is restored and the long chain C18 surface regions show again a lower friction than the short chain C7 regions.

The dependence of friction forces on the tip load has been studied for alkylsilanes of different chain length self-assembled on mica [8]. Up to load of 100 nN, elastic behavior was found and the frictional forces were always higher for the short chain molecules. Above a tip load of 100 nN, a substantial distortion of the alkylsilane chains was observed resulting in irreversible displacement of the molecules and damage of the organic film[8]. It is important to note that the situation is different for alkanethiols adsorbed on gold which undergo reversible displacement upon distortion at high loads. Atomic resolution imaging showed that the observed periodicity changed from a $(\sqrt{3}x\sqrt{3})R30°$ structure at low loads (repeatedly observed for thiol layers adsorbed on Au(111)) to a (1x1) structure at high load (due to the underlying Au(111)) and back to $(\sqrt{3}x\sqrt{3})R30°$ when the load was decreased again [18]. The mechanism underlying the observed behavior was unclear and three possibilities have been discussed. (i) desorption of the thiols at high loads and binding to the SFM tip, which are adsorbed to the gold again when the load is decreased; (ii) liquefying of the thiols under the tip pressure so that the tip penetrates the monolayers and images the gold; (iii) lateral displacement of the thiols, which are still adsorbed to the substrate[18]. Our findings exclude the first possibility since this mechanism would be expected to degrade the pattern quality, manifestly not the case here, as observed in Figure 3c. The same argument is true in a weaker sense for the second possibility since it is unlikely that the liquefied C18 and C7 molecules reassemble in a patterned ordered layer, especially at the phase boundaries. Thus some degradation of the pattern might be expected. However, the effect of liquefying the layer is likely to be felt quite locally, i.e. under the tip. We believe that the observation of an essentially unperturbed pattern is most consistent with the third possibility. The displacement is expected to be more difficult for the long chain molecules resulting in a higher friction which is experimentally observed (Figure 3b). This is also consistent with the differences observed between alkylsilanes on mica vis a vis thiols on gold: in the former case, the tip/monolayer interactions tend to be destructive at high force loadings while in the latter case, the monolayer more easily accommodates high pressure form the tip. This derives from the differences in structure between the two types of film: the lateral bonding in the silane-based layers implies that neighboring molecules are essentially connected to a perturbed molecule and thus moves together with it, while in the alkanethiol case the molecules are sufficiently mobile to readjust their positions under pressure.

CONCLUSIONS

We have shown that LFM and FMT provide excellent image contrast for patterned SAMs of alkanethiols of different chain lengths adsorbed on a gold substrate. The observed lower friction over the long chain surface regions correlates with a higher "softness" detected for the long chain regions by FMT. This is even true for a patterned SAM consisting surface regions of quite similar chain length , i. e. C18/C16. To clarify the role of the substrate as well as the effects of disorder and coverage complementary measurements, including spectroscopic methods, are in progress. The observation of a reversible image contrast reversal in the friction map as the applied load is increased and decreased again strongly supports an underlying mechanism in which the thiols are adsorbed to the substrate but laterally displaced/bent.

ACKNOWLEDGMENTS

G. B. wishes to thank the Deutsche Forschungsgemeinschaft (DFG) and the Los Alamos National Laboratory (LANL) for the financial support. Work at LANL was supported by the Department of Energy, Office of Basic Sciences and LANL Chemistry LDRD Funding. S. R. wishes to thank LANL for a Director's Funded Post-doctoral Fellowship.

REFERENCES

1. J. Seto, T. Nagai, C. Ishimoto and H. Watanabe, Thin Solid Films **160**, 453 (1985).
2. K. Deng, R. J. Collins, M. Mehregany and C. N. Sukenik, J. Electrochem. Soc. **142**, 1278 (1995).
3. I. Willner, R. Blonder and A. Dagan, J. Am. Chem. Soc. **116**, 9365 (1994).
4. A. Ulman, Introduction to Ultrathin Organic Films, (Academic Press, Inc., San Diego, 1991), pp. 339-362.
5. J. L. Wilbur, E. Kim, Y. Xia and G. M. Whitesides, Adv. Mat. **7**, 649 (1995).
6. T. J. Gardner, C. D. Friesbie and M. S. Wrighton, J. Am. chem. Soc. **117**, 6927 (1995).
7. R. M. Overney, E. Meyer, J. Frommer, H. J. Güntherodt, M. Fujihira, H. Takano and Y. Gotoh, Langmuir **10**, 1281 (1994).
8. X. Xiao, J. Hu, D. H. Charych and M. Salmeron, Langmuir **12**, 235 (1996).
9. C. D. Frisbie, L. F. Rozsnyai, A. Noy, M. S. Wrighton and C. M. Lieber, Science **263**, 2071 (1994).
10. J. L. Wilbur, H. A. Biebuyck, J. C. MacDonald and G. M. Whitesides, Langmuir **11**, 825 (1995).
11. M. Radmacher, R. W. Tillmann, M. Fritz and H. E. Gaub, Science **257**, 1900 (1992).
12. R. M. Overney, T. Bonner, E. Meyer, M. Rüetschi, R. Lüthi, L. Howald, J. Frommer, H.j. Güntherodt, M. Fujihira and H. Takano, J. Vac. Sci. Technol. B **12**, 1973 (1994).
13. A. Kumar and G. M. Whitesides, Appl. Phys. Lett. **63**, 2002 (1993).
14. This is an estimate only assuming a force constant of 0.1 N/m for the used cantilever according to the value provided by the manufacturer.
15. A. Noy, C. D. Frisbie, L. F. Rosznyai, M. S. Wrighton and C. M. Lieber, J. Am. Chem. Soc. **117**, 7943 (1995).
16. C. D. Bain, Troughton E. B., Y.-T. Tao, J. Evall, Whitesides, G. M. and R. G. Nuzzo, J. Am. Chem. Soc. **111**, 321 (1989).
17. M. D. Porter, T. B. Bright, D. L. Allara and C. E. D. Chidsey, J. Am. Chem. Soc. **109**, 3559 (1987).

etc...)[1,2] During the intervening years, the code has followed and sometimes nurtured the development of computing technology. Briefly, the first multipurpose code version, MCS, was written in 1963.[3] The first public release of the neutron photon code, MCNP was in the mid-70's.[4,5,6] The 1980's saw the release of MCNP3, MCNP3A, and MCNP3B which brought the code into standard Fortran and incorporated features such as generalized sources, repeated structures, criticality, multigroup option, and tally plotting. The 90's are the decade of version 4. MCNP4 was released in 1990 (MCNP4.2 was distributed from RSIC in 1991) and was specifically designed for UNIX operating systems. MCNP4 also included electron transport based upon the Integrated Tiger Series (ITS),[26] shared memory multitasking, thick target bremsstrahlung, and better random number control. MCNP4A was released in 1993 and included such features as dynamic memory allocation, X-window graphics, and distributed processor multiprocessing[35]. MCNP4B is expected to be released in about one year's time, 1997, and a few of its features will be presented later.

During the years of development the code system has been at the forefront of Monte Carlo methods and techniques, of experimental benchmarking and comparison, and of computer innovations and applications. Many innovations have been incorporated into the code after undergoing a thorough validation program; some, like those mentioned above, have withstood the test of time while others have not and have been eliminated (such as the ablility to run in obsolete operating systems or once more collided flux estimators.) Similarly, specific capabilities, such as importance sampling or weight window generation, have been implemented in such a way as to allow the skilled user to take advantage of them while not penalizing the neophyte. This constant improvement is a reflection of the MCNP philosophy of "Quality, Value and New Features" in action. The issue of quality is of paramount importance and will be discussed later with respect to software quality assurance. Put simply, quality means that the code and models are the best and most accurate available. Coupled closely to the quality component is the value component which is exemplified by extensive documentation and portability; the value is the usability of the code. Finally, we need new features to keep the code robust but new features never take precedence over quality or value.

Let me discuss quality assurance in more detail. The most important aspect of the MCNP code development effort is software quality assurance(SQA)[7]. This is evidenced in many ways but I will focus on a few which illustrate how features are incorporated in the code. First there is the validation of the capability or feature. Does the enhancement improve the code performance in actual problems while not conflicting with other existing capabilities? The validation effort requires an extensive set of code runs to be done and compared to experimental data or other independent runs to demonstrate that the feature is performing as expected. A typical suite of runs is illustrated by the validation of the differential operator technique reported by G. McKinney and J. Iverson in LA-13098[8,9] where over a hundred independent code runs were done to show that this new feature performed as expected and was consistent with previous results. Typically, this benchmarking effort is documented internally to Los Alamos with several detailed technical memoranda and a final Los Alamos technical report. Once documented, the feature undergoes multiple reviews before incorporation in the code. This evolutionary process reflects how the physics models have improved or numerical techniques have advanced, and we expect to see MCNP to continue to improve along these lines in the future.

Another important aspect of SQA is that the lines of codes are indeed performing as expected on any platform. This involves the test suite[10] which comes with the code and is derived from the validation runs and related experience. When the code is installed on any platform, it is required to give the same answers on a set of test problems; deviations indicate that there is an error in the installed code and it should be reinstalled or that there is another hardware/software problem. Hardware problems may have no significant impact on code accuracy but the test set usually catches most of these problems. Thus we require passing of all test problems for a successful installation. In point of fact this may sound pretty easy, but it actually has many subtleties. This subtlety is illustrated by a recent installation of MCNP on a 64-bit workstation with multiple processors.[11] Much of the hardware/software architecture was peculiar to that workstation, and was different from the 64 bit architecture of Cray mainframes. Moreover, the results from the test problems were not tracking. This problem uncovered a bug in the C code which impacted only the installation